

# Excitonic line broadening in PbSrSe thin films grown by molecular beam epitaxy

W. Z. Shen

Laboratory of Condensed Matter Spectroscopy and Opto-Electronic Physics, Department of Physics, Shanghai Jiao Tong University, 1954 Hua Shan Road, Shanghai 200030, People's Republic of China

H. Z. Wu and P. J. McCann

School of Electrical and Computer Engineering, Laboratory for Electronic Properties of Materials, University of Oklahoma, Norman, Oklahoma 73019-1023

(Received 17 September 2001; accepted for publication 12 December 2001)

Pb<sub>1-x</sub>Sr<sub>x</sub>Se thin films grown by molecular beam epitaxy have been investigated by x-ray diffraction and temperature-dependent photoluminescence measurements with the Sr composition as high as 0.276. Temperature and composition dependent excitonic line broadening effects in PbSrSe thin films have been studied on the basis of the proposed theoretical models and the experimentally obtained lattice constant, excitonic energy gap and effective mass as a function of the alloy composition. The exciton-longitudinal optical phonon coupling model has been employed successfully for PbSrSe with a coupling strength of 51.0 meV, which can be well explained by the proposed theoretical approach. The lattice deformation may have played a key role in the composition dependent broadening in PbSrSe at low temperature, rather than the normally observed alloy disorder effect in III-V and II-VI semiconductor materials. © 2002 American Institute of Physics. [DOI: 10.1063/1.1448897]

## I. INTRODUCTION

The growth of IV-VI lead chalcogenide semiconductors by molecular beam epitaxy (MBE) opens the possibility for novel optoelectronic devices, particularly useful for long wavelength infrared intrinsic detectors and mid-infrared lasers.<sup>1</sup> Alloying Sr into PbSe can significantly increase the band gap energy of Pb<sub>1-x</sub>Sr<sub>x</sub>Se, which is tunable from 0.28 eV to 3.60 eV at room temperature with  $x=0$  and 1, respectively. The material has a multivalley band structure with band extrema at the  $L$  point in  $\mathbf{k}$  space of the first Brillouin zone, and the band gap is at the four equivalent  $L$  points in the Brillouin zone. The absence of a heavy-hole band reduces the nonradiative Auger recombination rate, one or two orders of magnitude lower than that of narrow gap III-V and II-VI materials,<sup>2,3</sup> and influences favorably the high temperature threshold current. Lower density of states and stronger interband matrix elements allow the appearance of stimulated emission at relatively low generation rates. As a result, strong continuous-wave room temperature stimulated emission luminescence has been observed<sup>2,3</sup> between 3.0 and 4.0  $\mu\text{m}$  from PbSe/PbSrSe multiple quantum well (MQW) structures, well above the limit of 2.3  $\mu\text{m}$  in type II quantum cascade laser structures using narrow gap III-V antimonide semiconductor materials.

Photoluminescence (PL) is one of the best tools to study radiative relaxation phenomena and characterize thin film quality. We have revealed<sup>4</sup> that the exciton transitions are localized in PbSrSe with low Sr composition, and the excitons are separated into either free or trapped (strongly localized) excitons in high Sr composition PbSrSe films. Further on, high temperature (or even room temperature) excitonic effects allow very promising features, such as optical bista-

bility, four-wave mixing and large electro-optic coefficients.<sup>5</sup> PL technique especially allows one to investigate specific properties of materials such as PL excitonic line broadening due to the temperature and alloy disorder. Exciton-longitudinal optical (LO) phonon coupling plays an important role for the use of semiconductors and their quantum well (QW) structures as optoelectronic devices. The understanding of physical phenomena of excitonic line broadening in PbSrSe thin films is therefore of great interest for its laser and other device applications. In this paper, excitonic line broadening effects due to the temperature and alloy fluctuations have been studied in detail for MBE grown Pb<sub>1-x</sub>Sr<sub>x</sub>Se thin films with Sr compositions of as high as 0.276. The optical investigation in the literature is limited to the narrow band Pb<sub>1-x</sub>Sr<sub>x</sub>Se materials with the largest Sr composition of less than 0.1-0.2.<sup>1,6,7</sup> This enables us to obtain information on the excitonic lines and material parameters over much wide spectral range, due to the rapid increase in energy gap with the Sr composition.

## II. EXPERIMENTAL DETAILS

Three PbSrSe thin films were grown on freshly cleaved BaF<sub>2</sub> (111) substrates by MBE techniques in an Intevac GEN II Modular system. PbSe, Se, and Sr are used as source materials, and the Sr concentration in PbSrSe films can be determined from the beam equivalent pressure (BEP) ratios of the Sr and PbSe fluxes. A Sr-to-PbSe flux ratio of 2.9%, 7.4%, and 12.0% was employed to grow the three PbSrSe thin films. This results in Sr compositions of 0.066, 0.171, 0.276, respectively, based on the calibration of Lambrecht *et al.*<sup>1</sup> and about 12% BEP calibration error (within the uncertainty of the calibration<sup>1</sup>) due to the different concentra-

tion gradients across the sample holder in different MBE facilities.<sup>3,4</sup> The thin films have layer thickness of around 1  $\mu\text{m}$ . The temperature-dependent PL and absorption measurements for the PbSrSe thin films were performed on a Nicolet Nexus 870 Fourier transform infrared spectrometer (FTIR) with a liquid nitrogen cooled InSb detector and a 532 nm laser as the excitation source for PL and a global infrared source for absorption. The optical measurements were made at the resolution of 4  $\text{cm}^{-1}$ . The x-ray diffraction (XRD) measurements were carried out on a Shimadzu XD-3A system.

### III. THEORETICAL BACKGROUND

With the increase of temperature, the exciton transition in semiconductors is broadened by LO phonon scattering, and the temperature-dependent exciton linewidth ( $\Gamma$ ) can be described by the sum of the temperature-independent inhomogeneous term ( $\Gamma_i$ ) and the temperature-dependent homogeneous term ( $\Gamma_h$ ). The latter is the product of exciton–LO-phonon coupling strength ( $\Gamma_c$ ) and the LO-phonon population ( $N_{\text{LO}}$ ):

$$\Gamma = \Gamma_i + \Gamma_h, \quad \Gamma_h = \Gamma_c \cdot N_{\text{LO}} = \Gamma_c [\exp(\hbar\omega_{\text{LO}}/k_B T) - 1]^{-1} \quad (1)$$

with  $k_B T$  the thermal energy and  $\hbar\omega_{\text{LO}}$  the LO-phonon energy. Furthermore, the homogeneous linewidth  $\Gamma_h$  is directly related with the exciton radiation decay time ( $\tau_{\text{rad}}$ ), which has been theoretically proposed by Feldmann *et al.*<sup>8</sup> and experimentally demonstrated recently:<sup>9,10</sup>

$$\tau_{\text{rad}} \sim \Gamma_h [1 - \exp(-\Gamma_h/k_B T)]^{-1} \quad (2)$$

and it is obvious that the exciton–LO-phonon coupling is an important parameter for the use of semiconductors and their QW structures as optoelectronic devices, and is still a subject of considerable experimental and theoretical interest.<sup>8–12</sup>

A long wavelength LO phonon in a polar semiconductor produces an electrical field<sup>13</sup>

$$\mathbf{E}(\mathbf{r}) = -4\pi F \sum_{\mathbf{q}} \mathbf{e}_{\mathbf{q}} [a_{\mathbf{q}} \exp(i\mathbf{q} \cdot \mathbf{r}) + a_{\mathbf{q}}^+ \exp(-i\mathbf{q} \cdot \mathbf{r})], \quad (3)$$

where  $\mathbf{q}$  is the phonon wave vector,  $\mathbf{e}_{\mathbf{q}}$  is the polarization vector,  $a_{\mathbf{q}}$  and  $a_{\mathbf{q}}^+$  are the phonon annihilation and creation operators, respectively, and the constant  $F$  is given by<sup>14</sup>

$$F = [\hbar\omega_{\text{LO}}/8\pi\Omega] (1/\epsilon_{\infty} - 1/\epsilon_0)^{1/2} \cdot [(m_e^* m_h^*)/(2\mu\hbar^3\omega_{\text{LO}})]^{1/4}. \quad (4)$$

Here  $\Omega$  is the volume unit,  $\epsilon_{\infty}$  and  $\epsilon_0$  are the high frequency and static dielectric constants, respectively,  $\mu$ ,  $m_e^*$  and  $m_h^*$  are the exciton, electron, and hole effective masses, respectively. The relatively large size of a Wannier exciton makes the phonon highly polarizable, so the LO phonons couple strongly to the excitons, and the exciton–LO-phonon coupling Hamiltonian (Fröhlich Hamiltonian) can be expressed as<sup>13,15</sup>

$$\hat{H}_{\text{coup}} = \sum_{\mathbf{q}} \mathbf{e}_{\mathbf{q}} \{ a_{\mathbf{q}} V_{\mathbf{q}} [\exp(i\mathbf{q} \cdot \mathbf{r}_e) - \exp(i\mathbf{q} \cdot \mathbf{r}_h)] + a_{\mathbf{q}}^+ V_{\mathbf{q}}^+ [\exp(-i\mathbf{q} \cdot \mathbf{r}_e) - \exp(-i\mathbf{q} \cdot \mathbf{r}_h)] \}, \quad (5)$$

where the subscripts  $e$  and  $h$  represent the electrons and holes, respectively, and

$$V_{\mathbf{q}} = i4\pi e F/q, \quad (6)$$

with  $e$  being the free electron charge.

The exciton–LO-phonon coupling strength  $\Gamma_c$  is proportional to the square of the probability amplitude of the transition from the initial state  $|\alpha\rangle$  to the final state  $\langle\beta|$ ,

$$\Gamma_c \propto |\langle\beta|\hat{H}_{\text{coup}}|\alpha\rangle|^2, \quad (7)$$

and therefore it can be approximated as

$$\Gamma_c \propto |V_{\mathbf{q}}|^2 = 2\pi e^2 (1/\epsilon_{\infty} - 1/\epsilon_0) \times [(m_e^* m_h^*)\hbar\omega_{\text{LO}}/(2\mu)]^{1/2}/(\hbar q^2 \Omega). \quad (8)$$

On the other hand, in ternary alloy semiconductors, the scatter of the band-gap energy due to the statistical distribution of the two kinds of elements (here Pb and Sr in  $\text{Pb}_{1-x}\text{Sr}_x\text{Se}$ ) results in the broadening of the luminescence linewidth. The average numbers of Pb and Sr atoms within the excitonic volume are  $(1-x)KV_{\text{exc}}$  and  $xKV_{\text{exc}}$ , respectively, with  $K=4/d^3$  the cation density ( $d$  the lattice constant), and  $V_{\text{exc}}=4\pi a_{\text{exc}}^3/3$  the excitonic volume ( $a_{\text{exc}}$  the exciton radius). The alloy broadening can be obtained from the standard deviation of the alloy composition within the excitonic volume by assuming a Gaussian line shape, and is then given by

$$\delta E = 2(2 \ln 2)^{1/2} [3x(1-x)/(16\pi a_{\text{exc}}^3/d^3)]^{1/2} dE_g/dx, \quad (9)$$

where  $dE_g/dx$  is the change of the energy band gap with the alloy composition  $x$ .

### IV. RESULTS AND DISCUSSION

For a comparison of theories with experimentally observed temperature- and Sr composition-dependent excitonic broadening effects in PbSrSe thin films, it is better to have some important and sensitive (to composition) thin film parameters, such as lattice constant, the change of the energy band gap with the alloy composition  $x(dE_g/dx)$ , and effective mass, to be taken on the same material. The alloy composition, lattice constant, and the lattice mismatch strain can be detected nondestructively by the XRD measurements. Shown in the inset of Fig. 1 is the spectrum for a thin film of  $\text{Pb}_{0.934}\text{Sr}_{0.066}\text{Se}$  on  $\text{BaF}_2(111)$  substrate. Figure 1 shows the XRD results of lattice constant as a function of the Sr composition  $x$ , where a linear dependence of the lattice constant  $d$  as a function of  $x$  is found. This demonstrates that Vegard's law is valid in the  $\text{Pb}_{1-x}\text{Sr}_x\text{Se}$  alloy system with  $x$  up to at least 0.276:

$$d = 6.124 + 0.143x \text{ (\AA)} \quad (0 \leq x \leq 0.276) \quad (10)$$

with a regressive coefficient of 0.9986 and standard deviation of 0.0011. The composition coefficient of 0.143 is right between the reported value of 0.123 for  $0 \leq x \leq 0.23$  in Ref. 3 and 0.153 for  $0 \leq x \leq 0.10$  in Ref. 1, which in turn demonstrates the good accuracy of the composition from our MBE growth design and spectroscopic measurements. The lattice

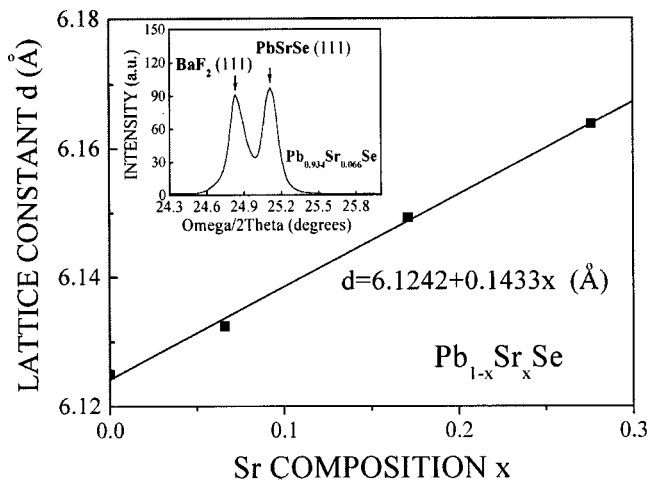


FIG. 1.  $Pb_{1-x}Sr_xSe$  lattice constant  $d$  as a function of the Sr composition  $x$  from x-ray diffraction measurements. The solid line is the linear fit result. Shown in the inset is the x-ray diffraction spectrum for a thin film of  $Pb_{0.934}Sr_{0.066}Se$  on  $BaF_2(111)$  substrate.

mismatch between the  $Pb_{1-x}Sr_xSe$  thin films and  $BaF_2(111)$  substrates is small:  $0.013-0.023x$  for  $0 \leq x \leq 0.276$ .

The excitonic band gap as well as the exciton linewidth as a function of temperature and composition  $x$  was determined from PL measurements. Typical PL spectra at 4.2 K of our samples are presented in Fig. 2 with the laser excitation intensity of  $1.0 \text{ W/cm}^2$ . Strong room temperature luminescence can be observed in  $Pb_{0.934}Sr_{0.066}Se$ , demonstrating the good quality of the sample. At low composition  $x$ , the low temperature spectra are dominated by single luminescence structure, which has been assigned to be the localized exciton (in alloy semiconductors) transition in  $PbSrSe$  based on a systematic study of the dependence of the luminescence spectra on the excitation intensity and temperature.<sup>4</sup> The excitonic line is separated into either free (at high energy side) or trapped (strongly localized at low energy side) excitons at

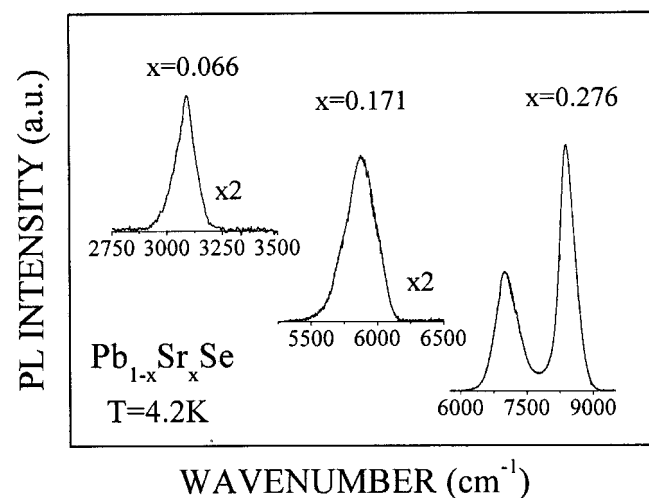


FIG. 2. Typical low temperature (4.2 K) photoluminescence spectra of  $Pb_{1-x}Sr_xSe$  thin films for different Sr composition  $x$ . Note the different scales in x axis.

low temperature due to the strong lattice distortions and alloy fluctuations under high Sr composition of 0.276 in  $PbSrSe$ .<sup>4,16</sup> A six-band  $k \cdot p$  model<sup>17</sup> has been employed to calculate the absorption edge from absorption measurements for the effective masses in  $PbSrSe$  thin films. The mass anisotropy ratio for ternary  $PbSrSe$  was estimated from these binary ones ( $m_{\parallel}/m_{\perp} = 1.8$  for  $PbSe$  and 3.0 for  $SrSe$ <sup>7</sup>) by using a linear interpolation scheme. The results for the effective masses parallel to the  $[111]$  direction  $m_{\parallel}$  is found to be

$$m_{\parallel}/m_0 = 0.3013 \times 10^{-3} (E_g/\text{meV}) + 0.00407 \quad (200 \leq E_g \leq 1200 \text{ meV}) \quad (11)$$

with  $m_0$  as the free electron mass and  $E_g$  the energy band gap. This expression is in good agreement with the results in Ref. 7 for small Sr composition, and  $PbSe$ <sup>18</sup> as well.

In order to know the exciton-phonon coupling in  $PbSrSe$  thin films, we show the full width at half maximum (FWHM) of the luminescence peak of  $Pb_{0.934}Sr_{0.066}Se$  thin film as a function of temperature in Fig. 3. The other two samples have similar behavior, which were not shown here. With the increase of temperature, the luminescence line shape gradually becomes increasingly asymmetric, and the transition gradually changes into band-to-band. In our experiments, reliable fits for the excitonic PL are possible only up to  $\sim 175 \text{ K}$ . In addition, we have also observed that the high-temperature slope decreases slightly with the Sr composition, indicating that phonon energy in  $PbSrSe$  increases slightly with the Sr composition (less than 2 meV with  $x$  of 0.276). We have used the exciton-LO-phonon coupling model by Eq. (1) to describe the exciton broadening. Since the LO-phonon energy for  $PbSrSe$  is not available now, we have approximately employed the value of  $PbSe$  of 16.8 meV<sup>19</sup> for the  $PbSrSe$  due to the small concentration of 0.066. A good fit is obtained with  $\Gamma_i$  of 12.8 meV and  $\Gamma_c$  of 51.0 meV, as the solid curve shown in Fig. 3. The accuracy for  $\Gamma_c$  is within  $\pm 2.0 \text{ meV}$ . The inhomogeneous linewidth  $\Gamma_i$

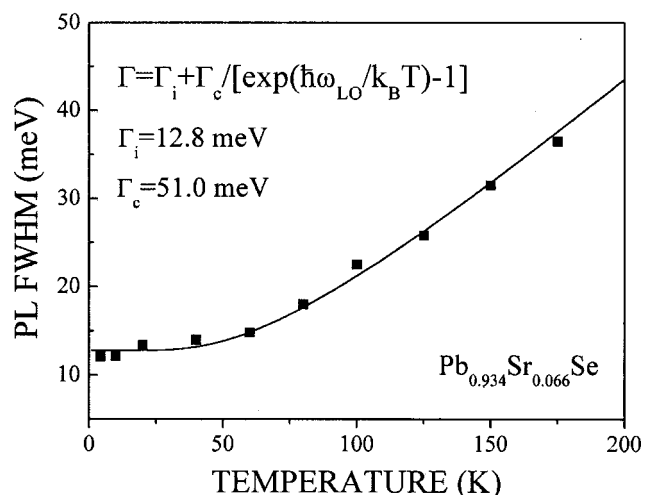


FIG. 3. Excitonic line broadening as a function of temperature in a  $Pb_{1-x}Sr_xSe$  thin film with the Sr composition  $x$  of 0.066. The solid curve is the calculated results from the exciton-LO phonon coupling model with the coupling strength  $\Gamma_c$  of 51.0 meV.

is mainly due to the alloy disorder and the film situation such as lattice deformation, interface roughness, misfit dislocations, etc., in the ternary PbSrSe thin film. Due to the large dielectric constant and small effective masses (absence of a heavy-hole band), the contribution of random-alloy disorder [from Eq. (9) in Sec. III] to the linewidth at low temperature is only 1.8 meV in  $\text{Pb}_{0.934}\text{Sr}_{0.066}\text{Se}$  (much smaller than  $\Gamma_i$  of 12.8 meV). This is in contrast to the case of III-V material where the random-alloy disorder dominates the inhomogeneous linewidth.<sup>11</sup> Considering the experimental facts of a relatively broad XRD peak (with the linewidth around 400 arcsec) and small lattice mismatch between the thin films and substrates, we attribute the inhomogeneous linewidth in PbSrSe is mainly related with the lattice deformation. Additional evidence for the exclusion of the effects of interface roughness and misfit dislocations is from the absorption and PL measurements (steep absorption edge and strong luminescence even at room temperature). This conclusion is further supported by the dependence of linewidth on Sr composition at low temperature shown below.

We note that the homogeneous broadening parameter  $\Gamma_c$  reported here is near twice that found in bulk GaAs layer,  $\Gamma_c(\text{GaAs})=30.4\pm 4.0$  meV.<sup>20</sup> The large difference of exciton-LO-phonon coupling between IV-VI and III-V materials can be well explained by the proposed theoretical approach of Eq. (8) in Sec. III, and is mainly due to a large difference of the parameters of  $\epsilon_\infty$ ,  $\epsilon_0$ ,  $m_e^*$ ,  $m_h^*$ , and  $\hbar\omega_{\text{LO}}$ . The above parameters for  $\text{Pb}_{0.934}\text{Sr}_{0.066}\text{Se}$  are relatively insensitive to the small composition of 0.066, and can be taken for approximation from these of PbSe except for the effective masses given by Eq. (11), and the parameters of both  $\text{Pb}_{0.934}\text{Sr}_{0.066}\text{Se}$  and GaAs are further approximated as being temperature independent. By employing the parameters of  $\epsilon_\infty=25.0$  (from Ref. 21),  $\epsilon_0=227.0$  (from Ref. 22),  $m_e^*\approx m_h^*=0.12m_0$  from Eq. (11),  $\hbar\omega_{\text{LO}}=16.8$  meV (from Ref. 19) for  $\text{Pb}_{0.934}\text{Sr}_{0.066}\text{Se}$ , and  $\epsilon_\infty=10.9$ ,  $\epsilon_0=12.9$ ,  $m_e^*=0.067m_0$ ,  $m_h^*=0.10m_0$ ,  $\hbar\omega_{\text{LO}}=36.8$  meV for GaAs (all from Ref. 23), we get  $\Gamma_c(\text{Pb}_{0.934}\text{Sr}_{0.066}\text{Se})/\Gamma_c(\text{GaAs})=2.0$ , in good agreement with the experimental results of  $\Gamma_c\sim 51.0\pm 2.0$  meV in  $\text{Pb}_{0.934}\text{Sr}_{0.066}\text{Se}$  and  $\Gamma_c\sim 30.4\pm 4.0$  meV in GaAs.<sup>20</sup>

The PL linewidth in PbSrSe thin films has also been studied as a function of Sr composition. The microscopic variation of the alloy composition strongly affects the linewidth of excitons in low temperature photoluminescence spectra (shown in Fig. 2) where thermal broadening effects are negligible. The calculated low temperature exciton PL broadening due to the alloy disorder from Eq. (9) with the material parameters in Eqs. (10) and (11), shown as the dotted curve in Fig. 4, is much smaller than those of the observed ones (filled squares). The alloy broadening effect itself cannot explain the full width at half maximum (FWHM) in the low temperature PL spectra of PbSrSe thin films, as well as the reported  $\text{Pb}_{0.953}\text{Sr}_{0.047}\text{Se}$  thin film ( $\sim 4.0$  meV at 10 K) in Ref. 7. This is quite understandable, since the excitons in PbSrSe are localized by the combined effects of the random alloy fluctuations and the lattice vibrations.

The rapid increase in PL linewidth with Sr composition  $x$  is mainly due to the increase in local lattice distortions

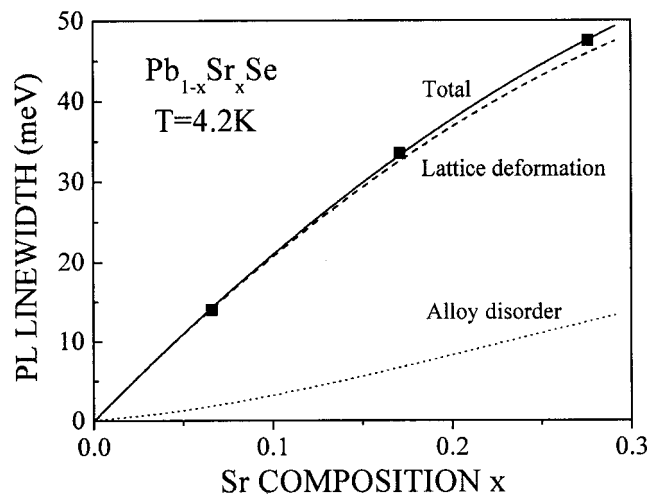


FIG. 4. Low temperature exciton PL linewidth in PbSrSe thin films as a function of Sr composition. Calculated results: dotted curve from alloy disorder contribution, dashed curve from lattice deformation contribution, and solid curve from the total contribution. Experimental results: filled squares.

around Sr atoms. This is clearly evident for the appearance of the broad luminescence band from self-trapped excitons at the low energy side of the  $\text{Pb}_{0.724}\text{Sr}_{0.276}\text{Se}$  PL spectrum (see Fig. 2) with a large Stokes shift of  $\sim 170$  meV. The increase in degree of the lattice deformation with composition  $x$  has also been observed in the XRD measurements, where the XRD peak linewidth increases with the Sr composition  $x$ . The exciton PL linewidth due to the lattice deformation can be roughly estimated in relation with the composition  $x$ . The degree of the crystal lattice deformation in the vicinity of Sr atoms can be approximately proportional to the product of Sr and Pb compositions  $x(1-x)$ , therefore, the contribution to the exciton PL linewidth is expected to be roughly linear with  $x(1-x)$ , as shown as the dashed curve in Fig. 4 with a scaling factor of 230 meV. The total contribution to the exciton PL linewidth (solid curve) from both the lattice distortions and the alloy disorder is in good agreement with the experiments, which clearly supports the assignment of the observed luminescence structures. The lattice deformation is found to have played a key role in the composition dependent broadening of PbSrSe thin films at low temperature, rather than the normally observed alloy disorder effect in III-V<sup>11,24</sup> and II-VI<sup>25</sup> semiconductor materials. One possible reason for the difference is that the local lattice distortion phenomenon happens easily in PbSrSe. This is due to the fact that elements Pb and Sr are from different groups (IV for Pb and II for Sr) with different outside electrons, rather than the elements from the same group in III-V (i.e.,  $\text{In}_x\text{Ga}_{1-x}\text{As}$ ) and II-VI (i.e.,  $\text{Cd}_{1-x}\text{Zn}_x\text{Te}$ ) materials.

## V. CONCLUSIONS

In summary, we have carried out x-ray diffraction and temperature-dependent photoluminescence measurements on MBE grown PbSrSe thin films for the study of excitonic line broadening effects. The lattice constant, excitonic energy gap, and effective mass as a function of the alloy composition were determined. A theoretical approach has been presented, which can well explain the observed large exciton-

LO-phonon coupling strength ( $\sim 51.0$  meV) from the temperature-dependent exciton–LO-phonon coupling model in PbSrSe thin films. However, we find that the lattice deformation in PbSrSe thin films may have played a key role in the composition dependent broadening at low temperature, rather than the normally observed alloy disorder effect in III–V and II–VI semiconductor materials. In addition, there is also controversy<sup>20</sup> on the exciton–LO-phonon coupling difference between the QW structures and their corresponding thin film materials recently. It is also of interest in studying the coupling in PbSe/PbSrSe MQW structures. Better understanding the coupling behavior is helpful for the application of semiconductor as well as its QW devices.

## ACKNOWLEDGMENTS

This work is supported in part by the Natural Science Foundation of China under Contract Nos. 10125416 and 60006005, Shanghai QMX and TRAPOYT of MOE, P.R.C. The authors would like to acknowledge Dr. X. G. Wang at National Laboratory for Infrared Physics, Chinese Academy of Sciences, L. F. Jian, L. G. Zhu, and Z. G. Qian at Shanghai Jiao Tong University for their technical help.

<sup>1</sup>A. Lambrecht, N. Herres, B. Spanger, K. Kuhn, H. Böttner, M. Tacke, and J. Evers, *J. Cryst. Growth* **108**, 301 (1991).

<sup>2</sup>P. J. McCann, K. Namjou, and X. M. Fang, *Appl. Phys. Lett.* **75**, 3608 (1999).

<sup>3</sup>X. M. Fang, K. Mamjou, I. N. Chao, P. J. McCann, N. Dai, and G. Tor, *J. Vac. Sci. Technol. B* **18**, 1720 (2000).

<sup>4</sup>W. Z. Shen, H. F. Yang, L. F. Jiang, K. Wang, G. Yu, and P. J. McCann, *J. Appl. Phys.* **91**, 192 (2002).

<sup>5</sup>D. S. Chemla, D. A. B. Miller, and P. W. Smith, in *Semiconductors and*

*Semimetals*, edited by R. Dingle (Academic, San Diego, 1987), Vol. 24, p. 279.

<sup>6</sup>G. Xu, X. M. Fang, P. J. McCann, and Z. Shi, *J. Cryst. Growth* **209**, 763 (2000).

<sup>7</sup>J. W. Tomm, K-P Möllmann, F. Peuker, K. H. Herrmann, H. Böttner, and M. Tacke, *Semicond. Sci. Technol.* **9**, 1033 (1994).

<sup>8</sup>J. Feldmann, G. Peter, E. O. Göbel, P. Dawson, K. Morre, C. Foxon, and R. J. Elliott, *Phys. Rev. Lett.* **59**, 2337 (1987).

<sup>9</sup>M. O'Neill, M. Oestreich, W. W. Rühle, and D. E. Ashenford, *Phys. Rev. B* **48**, 8980 (1993).

<sup>10</sup>R. Eccleston, B. F. Feuerbacher, J. Kuhl, W. W. Rühle, and K. Ploog, *Phys. Rev. B* **45**, 11403 (1992).

<sup>11</sup>W. Z. Shen, W. G. Tang, S. C. Shen, S. M. Wang, and T. G. Andersson, *Appl. Phys. Lett.* **65**, 2728 (1994).

<sup>12</sup>W. Z. Shen, S. C. Shen, W. G. Tang, Y. Chang, Y. Zhao, and A. Z. Li, *J. Phys.: Condens. Matter* **8**, 4751 (1996).

<sup>13</sup>A. V. Tulub, *Zh. Eksp. Teor. Fiz.* **34**, 1641 (1958).

<sup>14</sup>H. Fröhlich, *Adv. Phys.* **3**, 325 (1954).

<sup>15</sup>A. V. Tulub, *Zh. Eksp. Teor. Fiz.* **36**, 1859 (1959).

<sup>16</sup>C. D. Lee, H. L. Park, C. H. Chung, and S. K. Chang, *Phys. Rev. B* **45**, 4491 (1992).

<sup>17</sup>T. R. Globus, B. L. Gelmont, K. I. Gelman, V. A. Kondrashov, and A. V. Matveyenko, *Sov. Phys. JETP* **53**, 5 (1981).

<sup>18</sup>J. I. Pankove, *Optical Process in Semiconductors* (Dover, New York, 1975).

<sup>19</sup>R. Dalven, *Solid State Phys.* **28**, 179 (1973).

<sup>20</sup>A. V. Gopal, R. Kumar, A. S. Vengurlekar, A. Bosacchi, S. Franchi, and L. N. Pfeiffer, *J. Appl. Phys.* **87**, 1858 (2000).

<sup>21</sup>K. H. Herrmann, *Proc. SPIE* **3182**, 195 (1997).

<sup>22</sup>R. Klann, T. Höfer, R. Buhleier, T. Elsaesser, and J. W. Tomm, *J. Appl. Phys.* **77**, 277 (1995).

<sup>23</sup>D. Lee, A. M. Johnson, J. E. Zucker, R. D. Feldman, and R. F. Austin, *J. Appl. Phys.* **69**, 6722 (1991).

<sup>24</sup>W. Z. Shen, S. C. Shen, W. G. Tang, S. M. Wang, and T. G. Andersson, *J. Appl. Phys.* **78**, 1178 (1995).

<sup>25</sup>K. Oettinger, D. H. Hofmann, A.L. Efron, B. K. Meyer, M. Salk, and K. W. Benz, *J. Appl. Phys.* **71**, 4523 (1992).